Scanning Tunneling Microscopy Investigation of Silver Deposition upon Au(111) in the Presence of Chloride

4 AUTHORS, INCLUDING:

Seongpil Hwang

Korea University, Sejong, South Korea

31 PUBLICATIONS   **596** CITATIONS

Scanning Tunneling Microscopy Investigation of Silver Deposition upon Au(111) in the Presence of Chloride

Joohan Lee, Ilwhan Oh, Seongpil Hwang, and Juhyoun Kwak*

Department of Chemistry, Korea Advanced Institute of Science and Technology (KAIST), 373-1 Guseong-dong, Yuseong-gu, 305-701 Daejeon, Republic of Korea

Received April 30, 2002

Using electrochemical measurements and in situ scanning tunneling microscopy (STM), we confirm the process of Ag growth and the overlayer structures of Ag underpotential deposition (upd) on Au(111) in the presence or absence of chloride anions. There are four distinct structures of the Ag adlayer on Au(111) in the presence of chloride. Adlayer structures $(\sqrt{3} \times \sqrt{3})R30°$, $(\sqrt{19} \times \sqrt{19})R37°$, $(\sqrt{13} \times \sqrt{13})R46°$, and (6×6) are formed as a function of potential, and these structures are clearly matched to the features in a cyclic voltammogram. Compared with the (4×4) structure of Ag upd on Au(111) in a pure 0.1 M HClO$_4$ solution, overlayer structures of Ag on Au(111) in a chloride-containing solution are more loosely packed. Therefore, we conclude that the structures of the Ag overlayer on Au(111) strongly interact with chloride anions, suggesting the bilayer structure is composed of both Ag and Cl.

1. Introduction

Since the application of the scanning tunneling microscopy (STM) in an aqueous environment pioneered by Sonnenfeld and Hansma[1] in 1986, electrochemists have possessed abilities to observe a surface process with real-space images at the electrified solid−liquid interface. Using these abilities, multifarious results were reported about the reconstruction of metal surfaces,[2,3] the adsorption on metal surfaces,[4,5] corrosion,[6,7] and growth phenomena of metals,[8] which were all obtained under the potential control.[9,10] Among them, one of the most successful studies is the investigation of underpotential deposition (upd).[11,12] The research of upd systems triggers interests in fundamental as well as technical aspects such as catalysts,[13,14] thin-films,[15,16] sensors,[17] and the modification of metal surfaces.[18,19] Among the numerous upd systems that have been characterized, silver upd on gold is one of the most widely studied. Gewirth et al. reported the Ag upd on Au(111) by using in situ AFM, where the structure was dependent on the nature of the electrolyte. They observed a (3×3) adlayer of Ag upd in sulfate, a (4×4) overlayer in nitrate- and carbonate-containing electrolytes, and a complex structure in perchlorate after the first peak of Ag upd.[20−22] Unlike these, Itaya et al. found a $(\sqrt{3} \times \sqrt{3})R30°$ structure for the upd of Ag onto Au(111) in sulfate and a (4×4) overlayer in a perchlorate-containing solution posterior to the first upd peak.[23,24] The different results of each group may stem not only from the use of dissimilar tools (STM, AFM) but also from the effect of the trace amounts of contaminated anions. Especially, chloride may be one of the most serious interferences in the Ag upd system.

Using electrochemical techniques and X-ray photoelectron spectroscopy (XPS), Laibinis et al. showed that repetitive underpotential deposition and stripping of Ag on Au(111) in a sulfate solution with the trace amounts of chloride anions caused an increase of nobility of Ag upd.[25] They concluded that the transformation toward a much nobler Au(111) substrate resulted from the adsorption of chloride on silver during Ag upd and that of chloride on gold during stripping of an Ag adlayer, conceiving that halide ions strongly contribute to the formation of Ag adlayer structures. Therefore, two goals of our study of the Ag upd in the presence of halide are the investigation for a strong dependency on the counteranion in the overlayer structure and the definitive determination of the Ag adlayer structure in pure sulfate- or perchlorate-including electrolytes. However, there is no research about Ag upd onto Au(111) in the presence of halide anions such as chloride and iodide because of the low solubility of silver halide salts in aqueous media and other solvents.

In this paper, we report several stepwise stages of Ag growth and of atomic Ag structures on Au(111) in the

* Corresponding author. Fax: +82-42-869-2810. E-mail: jhkwak@kaist.ac.kr.

(1) Sonnenfeld, R.; Hansma, P. K. *Science* **1986**, *232*, 211.
(2) Coulman, D. J.; Wintterlin, J.; Behm, R. J.; Ertl, G. *Phys. Rev. Lett.* **1990**, *64*, 1761.
(3) Gao, X.; Weaver, M. J. *Phys. Rev. Lett.* **1994**, *73*, 846.
(4) Schardt, B. C.; Yau, S.-L.; Rinaldi, F. *Science* **1989**, *243*, 1050.
(5) Yau, S.-L.; Vitus, C. M.; Schardt, B. C. *J. Am. Chem. Soc.* **1990**, *112*, 3677.
(6) Fan, F.-R. F.; Bard, A. J. *J. Electrochem. Soc.* **1989**, *136*, 166.
(7) Oppenheim, I. C.; Trevor, D. J.; Chidsey, C. E. D. *Science* **1991**, *254*, 687.
(8) Sonnenfeld, R.; Schardt, B. C. *Appl. Phys. Lett.* **1986**, *49*, 1172.
(9) Gewirth, A. A.; Niece, B. K. *Chem. Rev.* **1997**, *97*, 1129.
(10) Herrero, E.; Buller, L. J.; Abruña, H. D. *Chem. Rev.* **2001**, *101*, 1897.
(11) Magnussen, O. M.; Hotlos, J.; Nichols, R. J.; Kolb, D. M.; Behm, R. J. *Phys. Rev. Lett.* **1990**, *64*, 2929.
(12) Manne, S.; Hansma, P. K.; Massie, J.; Elings, V. B.; Gewirth, A. A. *Science* **1991**, *251*, 183.
(13) Kolb, D. M. In *Advances in Electrochemistry and Electrochemical Engineering*; Gerischer, H., Tobias, C. W., Eds.; Wiley: New York, 1978; Vol. 11, pp 125−271.
(14) Adžić, R. R. In *Electrocatalysis*; Lipkowski, J., Ross, P. N., Eds.; Wiley-VCH: New York, 1998; pp 197−242.
(15) Sieradzki, K.; Brankovic, S. R.; Dimitrov, N. *Science* **1999**, *284*, 138.
(16) Hwang, S.; Oh, I.; Kwak, J. *J. Am. Chem. Soc.* **2001**, *123*, 7176.
(17) Michalitsch, R.; Laibinis, P. E. *Angew. Chem., Int. Ed.* **2001**, *40*, 941.
(18) Hsieh, M.-H.; Chen, C.-H. *Langmuir* **2000**, *16*, 1729.
(19) Baker, M. V.; Jennings, G. K.; Laibinis, P. E. *Langmuir* **2000**, *16*, 3288.

(20) Chen, C.-H.; Vesecky, S. M.; Gewirth, A. A. *J. Am. Chem. Soc.* **1992**, *114*, 451.
(21) Chen, C.-H.; Gewirth, A. A. *Ultramicroscopy* **1992**, *42−44*, 437.
(22) Mrozek, P.; Sung, Y.-E.; Han, M.; Gamboa-Aldeco, M.; Wieckowski, A.; Chen, C.-H.; Gewirth, A. A. *Electrochim. Acta* **1995**, *40*, 17.
(23) Hachiya, T.; Itaya, K. *Ultramicroscopy* **1992**, *42−44*, 445.
(24) Ogaki, K.; Itaya, K. *Electrochim. Acta* **1995**, *40*, 1249.
(25) Michalitsch, R.; Palmer, B. J.; Laibinis, P. E. *Langmuir* **2000**, *16*, 6533.

presence/absence of chloride. Because we could not overcome the inherently low solubility of AgCl, we used a low concentration of Ag^+ ions ($\sim 10^{-5}$ M).[26] Since the underpotential deposition of metal adatoms on a metal substrate is a thermodynamic process, which is associated with work functions of an adatom and a substrate, we deduce that the concentration 10^{-5} M must be acceptable. We expect that our observations will accelerate studies of metal upd systems in the presence of halide, which are less investigated because of the poor solubility of metal halide salts in water.

2. Experimental Section

Materials. The working electrode for electrochemical measurements was an Au(111) single crystal (MaTeck, Germany) with a diameter of 1 cm and a nominal area of 0.785 cm^2. For STM imaging, Au (thickness 250 ± 50 nm) substrates evaporated onto glass with Cr-adhesion layers (thickness ~ 3 nm) were obtained from Metallhandel Schroer GmbH, Germany. All Au electrodes were annealed for 3 min in a hydrogen flame prior to use and slowly cooled in air, following a published procedure.[27] Oxide formation and stripping voltammetry of the surface in pure electrolyte were found to closely match the literature for an Au(111) surface.[28] Electrochemical solutions were prepared from ultrapure water (Modulab, US Filter, MA, >18 MΩ). AgClO₄·H₂O (99.999%), AgCl (99.999%), and HClO₄ (double-distilled) were all obtained from Aldrich. A chloride-containing solution was prepared by sonicating AgCl salts for at least 3 h (Branson Ultrasonics Co.) because of the low solubility. This solution was saturated with Ag^+ and Cl^- ions of $\sim 10^{-5}$ M concentration.

Electrochemical Measurements. Cyclic votammetry was acquired using a Pt (99.99%, 0.5-cm diam, Aldrich) wire as a counter electrode and a saturated mercury–mercurous sulfate electrode (MSE) as a reference electrode connected to the electrochemical compartment via a capillary salt bridge to lessen contamination from the reference electrode. All potentials in this paper are quoted relative to the MSE (0.64 V vs NHE). The solutions were purged with Ar prior to use, and the atmosphere of an electrochemical cell was blanketed with Ar during all electrochemical measurements. Potential control and sweeps were conducted with an Autolab potentiostat (PGSTAT 10, Eco Chemie, Netherlands).

Scanning Tunneling Microscopy. STM images were collected in a constant current mode with Topometrix TMX 2000. A silver wire (99.99%, 0.5-cm diam, Aldrich) was employed for the reference electrode, while a Pt wire was used as the counter electrode. The scanner was calibrated against the lattice spacing of a highly ordered pyrolytic graphite (HOPG) surface in air for in-plane dimensions and against monatomic Au(111) steps for dimensions normal to the surface. The scanner was always stabilized for half a day to minimize thermal or acoustic vibrations before STM imaging and x, y, z-calibration. An electrochemically etched Pt/Ir wire (Molecular Imaging, AR) coated with Apiezon wax or polyethylene was used as the STM tip. All images are presented as unfiltered forms.

3. Results and Analysis

3.1. Electrochemical Measurements. *3.1.1. In the Absence of Cl⁻.* Figure 1 shows a cyclic voltammogram and a coulometric curve (inset) of Ag upd on an Au(111) single crystal in 1 mM AgClO₄ and 0.1 M HClO₄. This voltammetry and the corresponding coulometric curve are nearly identical to those in the previous work.[24] A first cathodic peak (C_1) appears at 0.560 V, and the corresponding anodic peak (A_1) is observed at 0.570 V. Another cathodic peak (C_2) is seen at −0.007 V with a shoulder

(26) Martell, A. E.; Smith, R. M. *Critical Stability Constants*; Plenum Press: New York, 1976; Vol. 4.

(27) Will, T.; Dietterle, M.; Kolb, D. M. In *Nanoscale Probes of the Solid–Liquid Interface*; Gewirth, A. A., Siegenthaler, H., Eds.; NATO ASI Series E; Kluwer Academic: Dordrecht, 1995; Vol. 288, p 137.

(28) Angerstein-Kozlowska, H.; Conway, B. E.; Hamelin, A.; Stoicoviciu, L. *J. Electroanal. Chem.* **1987**, *228*, 429.
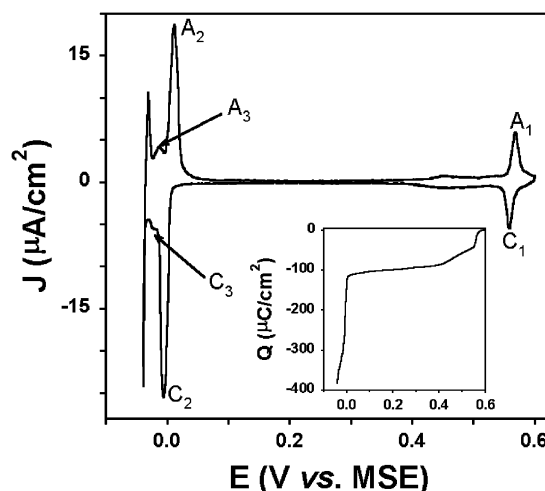

Figure 1. Cyclic voltammogram in 1 mM AgClO₄ and 0.1 M HClO₄ on an Au(111) single crystal. Scan rate = 2 mV/s. Inset: a coulometric curve corresponding to the cyclic voltammogram during a cathodic sweep.

peak (C_3) at −0.025 V. The reversible desorption (A_2) of the second Ag upd occurs at 0.011 V with a shoulder peak (A_3) at −0.014 V. This pair of shoulders (C_3 and A_3), not previously reported, is highly reversible. After the third peak of Ag upd, the cathodic current suddenly increases at −0.04 V, denoting the commencement of bulk Ag deposition. All features in this voltammogram are stable during several cycles, confirming that alloy formation between Ag and Au in the upd region does not occur.

A coulometric curve during Ag deposition is shown in the inset of Figure 1. To deposit a monolayer of Ag on Au(111), the charge density 222 $\mu C/cm^2$ is required under the assumption that the deposition of Ag is a process of one electron-transfer per silver ion. The amounts of charge density up to the C_1, C_2, and C_3 peaks within the Ag upd region are 46, 298, and 345 $\mu C/cm^2$, respectively. The amounts of surface coverage up to the C_1, C_2, and C_3 peaks are 0.21, 1.34, and 1.55, respectively. A monolayer of Ag is completed at −0.002 V around the C_2 peak, while a total value of 1.55 connotes that the second adlayer of Ag on Au(111) is present.

3.1.2. In the Presence of Cl⁻. Figure 2 shows a cyclic voltammogram and the corresponding coulometric curve (inset) obtained in a 0.1 M HClO₄ solution with saturated AgCl on an Au(111) single crystal. Five sets of adsorption and desorption peaks conform to several typical stages of Ag upd onto Au(111). A cathodic peak (C_1) of the first Ag upd begins to increase at 0.5 V and is split into two peaks that are observed at 0.475 and 0.398 V. The corresponding anodic peak (A_1) starts to increase at 0.400 V and is also divided into two peaks which occur at 0.438 and 0.519 V. When the potential changed to 0.63 V, an Au(111) electrode surface was oxidized, yielding a specific voltammetric response that was substantially identical to that observed in a pure HClO₄ solution.[29] This verifies that the aforementioned set of peaks (C_1 and A_1) corresponds to the first adsorption and desorption of Ag on the Au(111) electrode.

The cathodic peaks of C_2, C_3, and C_4 for deposition are shown at 0.095, −0.031, and −0.105 V, while the corresponding anodic peaks of A_2, A_3, and A_4 for stripping emerge at 0.166, 0.017, and −0.029 V, respectively. The differences between the cathodic peak potentials and the anodic peak potentials for the three series of peaks (C_2

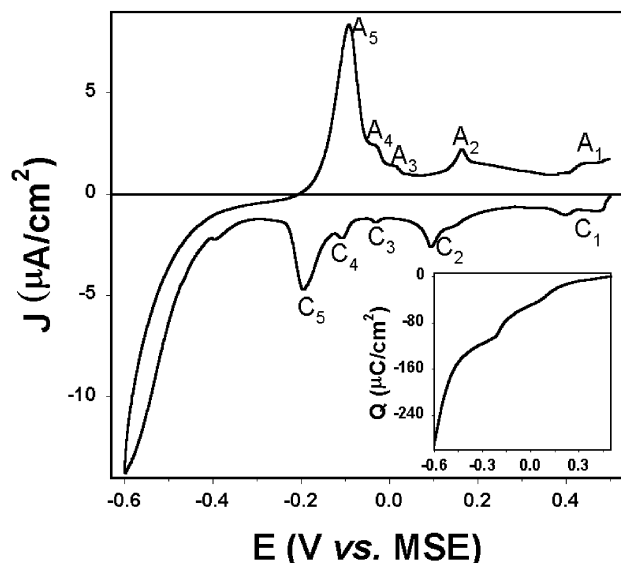(29) Hamelin, A. *J. Electroanal. Chem.* **1996**, *407*, 1.

Figure 2. Cyclic voltammogram in saturated AgCl and 0.1 M HClO₄ on an Au(111) single crystal. Scan rate = 2 mV/s. Inset: a coulometric curve corresponding to the cyclic voltammogram during a cathodic sweep.

and A$_2$, C$_3$ and A$_3$, C$_4$ and A$_4$) are 0.071, 0.048, and 0.076 V, respectively. This peak separation points out the irreversible behavior of Ag upd onto Au(111) in the presence of chloride, compared with nearly symmetric peaks in Ag upd in the absence of chloride (see Figure 1). These results may be due to the low concentration of Ag$^+$ ions and the competitive adsorption/desorption of chloride anions. In the bulk deposition realm, there are two distinctive regions. The deposition of Ag occurs at −0.194 V (C$_5$), and the additional deposition appears posterior to −0.4 V. The corresponding stripping peak of Ag (A$_5$) is seen at −0.090 V. As a control experiment, cyclic voltammetry was conducted in a pure HClO₄ solution in which it exhibited no distinct feature and only double-layer charging currents over the entire potential range shown in Figure 2. Thus, the peaks seen in Figure 2 are plainly appointed to the combined adsorption/desorption of silver and chloride.

　　The inset in Figure 2 displays a coulometric curve obtained from a cyclic voltammogram during a cathodic sweep. The amounts of charge density were intergrated and found to be 6, 46, 58, 70, and 109 μC/cm^2 for C$_1$, C$_2$, C$_3$, C$_4$, and C$_5$ peaks, respectively, with the total charge density of 290 μC/cm^2 to the limit of −0.6 V. The amounts of surface coverage for C$_1$, C$_2$, C$_3$, C$_4$, and C$_5$ peaks are 0.03, 0.21, 0.26, 0.32, and 0.49, respectively, with the total surface coverage of 1.31 prior to hydrogen evolution at −0.6 V. On the basis of charge calculations, the formation of one monolayer of Ag is not possible within the range of Ag upd. Thus, a monolayer of Ag is completed at −0.55 V after passing the C$_5$ peak.

　　3.2. STM Imaging of Ag Growth on Au(111). To estimate nucleation and growth behaviors of Ag, Ag-modified Au(111) electrodes were imaged by in situ STM when chloride was absent or present. Especially, chloride adsorption on an Au(111) substrate or an Ag layer induces the enhancement of surface mobility and the fluctuation of step sites.[30,31]

　　3.2.1. Ag Growth on Au(111) in the Absence of Cl$^-$. Figure 3 shows consecutive STM images of an Au(111) electrode under various potentials in 1 mM AgClO₄ and 0.1 M HClO₄.
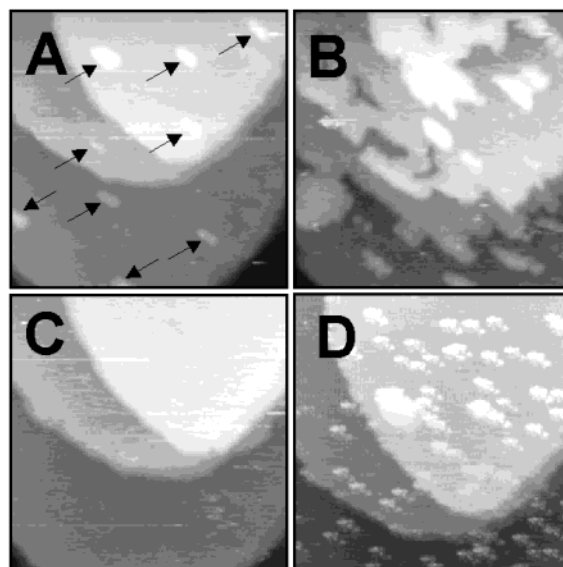
(30) Giesen, M.; Kolb, D. M. *Surf. Sci.* **2000**, *468*, 149.
(31) Dietterle, M.; Will, T.; Kolb, D. M. *Surf. Sci.* **1995**, *327*, L495.

Figure 3. 190 × 190 nm^2 STM images in a solution containing 1 mM AgClO₄ and 0.1 M HClO₄. (A) STM image of Ag islands on Au(111) terraces at E = 0.46 V. I_{tip} = 2 nA. E_{bias} = 200 mV. Arrows indicate Ag islands. (B) Lateral growth of Ag on Au-(111) terraces at E = 0.01 V. I_{tip} = 2 nA. E_{bias} = 650 mV. (C) A complete monolayer of Ag on Au(111) at E = −0.02 V. I_{tip} = 2 nA. E_{bias} = 680 mV. (D) The second Ag islands on Au(111) at E = −0.035 V. I_{tip} = 3 nA. E_{bias} = 700 mV.

At potentials positive of 0.61 V, STM images exhibit distinctive Au(111) terraces and steps. As the potential is moved to more negative values, the size of the islands becomes larger, and the lateral growth of Ag is more pronounced. Figure 3A displays an STM image of Ag islands on Au(111) obtained at 0.46 V. The islands on Au(111) terraces are assigned to Ag, since no island is observed in a pure HClO₄ solution at this potential. The positions of the Ag island (see arrows in Figure 3A) on an Au(111) substrate are exactly in accord with those of the gold island which arises from the lifting of the thermally induced surface reconstruction of Au(111) at positive potentials.[32] The measured heights of the Ag islands are 0.17 ± 0.02 nm, which are lower than a monatomic high step of 0.24 nm for an Ag(111) substrate. This height does not change up to the second peak (C$_2$) of Ag upd, as seen in Figure 1. At 0.045 V, additional Ag is deposited, and Ag islands begin to laterally grow at the step-edge sites of previously deposited Ag islands or an Au(111) substrate. Figure 3B shows the lateral growth of Ag obtained at 0.01 V. The height of the Ag adlayer is measured to be 0.24 ± 0.02 nm, which is in good agreement with that of a Ag-(111) step. As the potential becomes −0.02 V, Au(111) terraces are entirely covered with Ag, and a full monolayer of Ag onto Au(111) is accomplished, as shown in Figure 3C. Similar to the case of the previous work,[33] Figure 3D exhibits the second adlayer of Ag obtained at −0.035 V. The measured heights of the second overlayer above a monolayer of Ag are 0.17 ± 0.02 and 0.24 ± 0.03 nm, revealing that the Ag island shown in Figure 3A and an Ag island with a monatomic high step coexisted. At a potential close to −0.04 V, the bulk deposition of Ag starts, but the additional growth is not easily observed because of a shielding effect by an STM tip. When the potential becomes positive, reversely, stripping of Ag commences, and terraces and steps of an Au(111) surface reappear.

(32) Dakkouri, A. S. *Solid State Ionics* **1997**, *94*, 99.
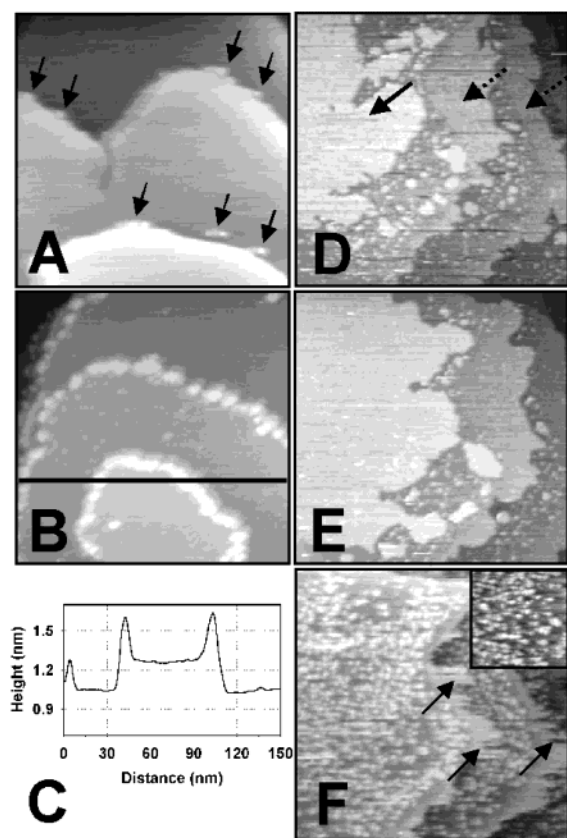(33) Esplandiu, M. J.; Schneeweiss, M. A.; Kolb, D. M. *Phys. Chem. Chem. Phys.* **1999**, *1*, 4847.

Figure 4. STM images in a solution consisting of saturated AgCl and 0.1 M HClO$_4$. (A) 170×170 nm^2 image of Ag nucleation at Au(111) steps at $E = 0.17$ V. $I_{tip} = 1$ nA. $E_{bias} = 200$ mV. (B) 150×150 nm^2 image of Ag decoration on Au(111) step sites at $E = -0.12$ V. $I_{tip} = 2$ nA. $E_{bias} = 400$ mV. (C) The line profile of Ag decoration at Au(111) steps along the line marked in part B. (D) 180×180 nm^2 image of Ag growth on Au(111) terraces at $E = -0.38$ V. $I_{tip} = 1$ nA. $E_{bias} = 500$ mV. A solid-lined arrow points out an Ag island deposited on an Au(111) terrace. Dash-lined arrows designate Ag growth at the upper and outer steps of an Au substrate. (E) 180×180 nm^2 image of a monolayer of Ag on Au(111) at $E = -0.53$ V. $I_{tip} = 1$ nA. $E_{bias} = 600$ mV. (F) 180×180 nm^2 image of AgCl complexes after the potential step from -0.53 to -0.18 V. $I_{tip} = 1$ nA. $E_{bias} = 300$ mV. Inset: 70.6×70.6 nm^2 image of AgCl clusters on an Au(111) terrace at $E = 0.12$ V. $I_{tip} = 1$ nA. $E_{bias} = 200$ mV.

Therefore, Ag adsorption and desorption on Au(111) in a pure HClO$_4$ solution are quite reversible processes which are supported by a series of symmetric peaks, as displayed in Figure 1.

3.2.2. Ag Growth on Au(111) in the Presence of Cl$^-$. Figure 4A shows an STM image of Ag upd on Au(111) in 0.1 M HClO$_4$ and saturated AgCl obtained at 0.17 V. Ag islands are exclusively deposited around defects such as Au(111) steps, which are designated by arrows. It is interesting that Ag adsorbs only the lower portion of an Au(111) step, evincing that the lower part of the step is energetically more favorable than the upper part of the step. For comparison, STM images are obtained in pure 0.1 M HClO$_4$ at potentials between 0.0 and 0.5 V, in which any island is not found, indicating that the arrowed bright spots in Figure 4a are definitely Ag islands. The heights of the Ag islands are measured to be 0.34 ± 0.02 nm, which are much higher than that of an Ag upd island in the absence of chloride, which might be analyzed to maintain the bilayer structure composed of silver and chloride. Also, this bilayer structure of Ag and Cl rapidly moves toward a step-edge of Au(111), and it forms bumps

at a step, which reveals the increase of surface mobility by chloride adsorption.[34]

As the potential is moved to -0.12 V, decorated Au-(111) steps by additional Ag deposition are clearly seen in Figure 4B. The edge decoration of Au(111) steps is evenly distributed at all steps of an Au(111) substrate, which was also observed for Cu upd on Au(111).[35] This feature indicates that the diffusion-limited control mainly dominates the Ag growth, and silver at low concentration favors the energetically most stable site, such as a step. The deposition at local step sites is more clearly visualized in the profile in Figure 4C, which is taken along the line marked in Figure 4B. The height of the edge decoration is measured to be 0.36 ± 0.03 nm, which denotes another adlayer on the predeposited Ag upon an Au(111) substrate. To investigate the role of chloride more deeply, an Au-(111) substrate was imaged in a pure HClO$_4$ solution only with Ag$^+$ ions at 10^{-5} M but evenly decorated Au(111) steps such as those in Figure 4B were hardly observed in the absence of chloride. Therefore, the equal distribution of Ag islands at Au(111) steps suggests that the chloride adsorption plays a significant role in edge decoration.

Figure 4D displays an STM image of Ag-deposited Au-(111) terraces obtained at -0.38 V. A large Ag island, designated by a solid-lined arrow, and a bunch of small islands are distinctly seen with the highest brightness. In the closely zoomed in Ag islands, there are many pits, demonstrating that the Ag adlayers are loosely packed and are coalescing during a growth process. The upper and outer parts of the Au(111) steps (see dash-lined arrows in Figure 4D) are much brighter than the inner Au(111) terrace, indicating the maintenance of the edge decoration at the Au(111) steps. Also, horizontally grown bumps shown at step sites represent the lateral growth of Ag. A full monolayer of Ag and additional Ag islands on an Au-(111) surface are obviously observed at -0.53 V in Figure 4E when the charge density is 210 μC/cm^2, as described in the inset of Figure 2. The Ag overlayer keeps a similar morphology to that of the image in Figure 4D, which reconfirms the lateral growth of Ag. The height between steps is measured to be 0.24 ± 0.02 nm, which is a monatomic high step of a Ag(111) surface.

Unlike those mentioned above, STM images were collected when the potential was positively changed. Figure 4F exhibits an STM image when the potential was stepped to -0.18 V after the acquisition of an STM image in Figure 4E. Under this condition, the surface of an Ag adlayer is substantially rough, numerous particle-like islands are formed, and the step sites of a substrate are fluctuated. Primitively, these results were surprising and were not easily understood. However, the existence of chloride reveals a clue to untie these entanglements. As the potential was stepped to the positive value, the predeposited Ag adlayer was stripped, the desorbed Ag$^+$ ions were combined with chloride anions adsorbed on the Ag adlayer or with chloride anions in solution, and AgCl was finally formed on Au(111). The AgCl with a particle shape is uniformly distributed upon the bare Au(111), and the vertical distance of these particles is measured to be 0.35 ± 0.02 nm, supporting the formation of AgCl. These particles firmly adhere to an Au(111) surface even if the potential is stepped to 0.12 V, which is more clearly visualized in the inset of Figure 4F. Compared with the stripping of the Ag adlayer in pure electrolytes only with Ag$^+$ ions, the AgCl desorption requires more overpotential,

(34) Wiechers, J.; Twomey, T.; Kolb, D. M.; Behm, R. J. *J. Electroanal. Chem. Interfacial Electrochem.* **1988**, *248*, 451.

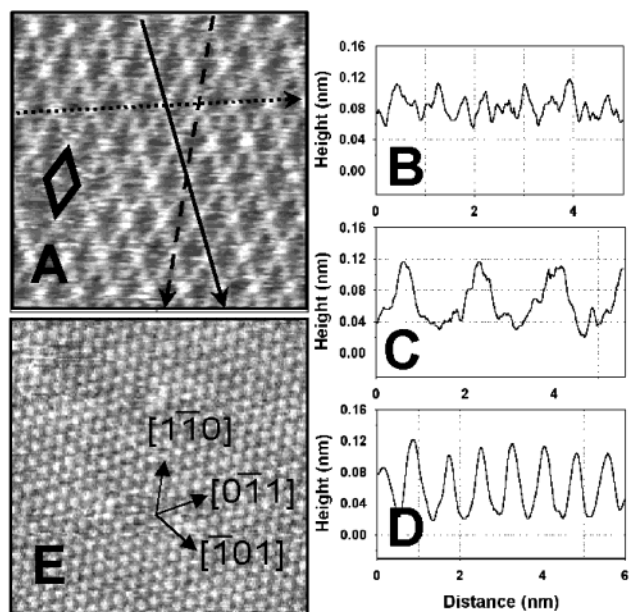(35) Kolb, D. M. *Angew. Chem., Int. Ed.* **2001**, *40*, 1162.

Figure 5. (A) 6.46×6.46 nm^2 image of an Ag adlayer on Au-(111) in 1 mM AgClO$_4$ and 0.1 M HClO$_4$ at $E = 0.36$ V. $I_{tip} = 2$ nA. $E_{bias} = 350$ mV. The unit cell of a (4×4) structure is indicated with a rhombus. The line profiles along a solid-lined (B), a dash-lined (C), and a dot-lined (D) arrow are marked in Figure 5A. (E)Atom-resolved STM image $(5.73 \times 5.73$ nm$^2)$ of a close-packed (1×1) adlayer at $E = 0.006$ V. $I_{tip} = 2$ nA. $E_{bias} = 610$ mV. The lattice vectors are denoted with arrows and notations.

indicating that the processes of Ag adsorption and desorption on Au(111) in the presence of chloride anions are irreversible. The AgCl does not disappear until the potential becomes 0.35 V, and a smooth surface is disclosed again at this potential realm. In addition to the formation of AgCl, the adsorption of chloride at step sites induces the growth of streaky steps, manifested by arrows in Figure 4F, and the fluctuation of step-edges by the enhancement of surface mobility, as described in the previous report.[31]

3.3. Atom-Resolved STM Images of Ag Deposition on Au(111). To confirm the adlayer structures of Ag upd on Au(111) in a HClO$_4$ solution with or without Cl$^-$ ions, we performed atom-resolved STM measurements on each system in the underpotential region, and various overlayer structures of Ag on Au(111) were reproducibly obtained in the presence or absence of chloride.

3.3.1. STM Imaging of Ag Upd on Au(111) in the Absence of Cl$^-$. Figure 5A shows an atomic STM image of an open Ag structure obtained at 0.36 V posterior to the first Ag upd in 1 mM AgClO$_4$ and 0.1 M HClO$_4$. The distance between the brightest spots (a moiré pattern) is measured to be 1.15 ± 0.05 nm, which is 4 times longer than the interatomic distance of an Au(111) surface. Since the lattice vectors of this structure are aligned with atomic rows of Au(111), the adlayer structure of Ag on Au(111) must be a (4×4) adlattice, and the unit cell is designated in Figure 5A with a rhombus. This structure is identical to that in the previous work,[24] validating that our in situ STM is reasonable to attain structural information in detail. The corrugated modulation of a (4×4) adlattice is more substantially presented in the profile with two kinds of atomic modulations of 0.06 and 0.03 ± 0.01 nm above the corresponding terrace in Figure 5B, which is taken along the solid-lined arrow marked in Figure 5A. To acquire further information, Figure 5C clearly displays another line profile of an Ag adlayer with the heights of
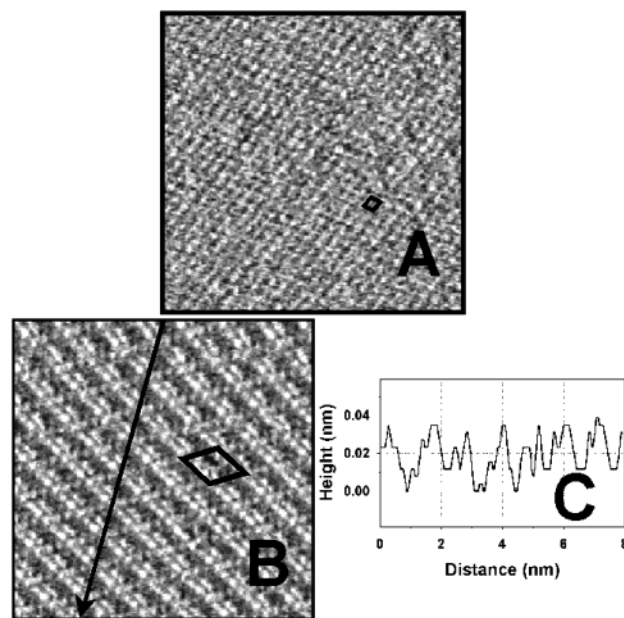

Figure 6. (A) STM image of a 7.6×7.6 nm^2 area in saturated AgCl and 0.1 M HClO$_4$ at $E = 0.4$ V. $I_{tip} = 2$ nA. $E_{bias} = 200$ mV. The unit cell of a $(\sqrt{3} \times \sqrt{3})$R30° structure is designated. (B) 9.5×9.5 nm^2 image of an Ag adlayer on Au(111) at $E = 0.2$ V. $I_{tip} = 2$ nA. $E_{bias} = 400$ mV. A unit cell is indicated with a rhombus. (C) Profile along the solid-lined arrow drawn in part B.

0.08, 0.04, and 0.02 ± 0.01 nm along the dash-lined arrow, and Figure 5D shows a line profile along the dot-lined arrow, in which the vertical distance is measured to be 0.10 ± 0.02 nm. These modulations elucidate that Ag adatoms are landed at different positions of an Au(111) surface. Ag adatoms with a strong moiré pattern are sat atop sites of Au(111) atomic rows, while Ag atoms with less bright spots are positioned on 2-fold or 3-fold hollow sites.

As the potential moves to the second Ag upd region, a new atomic structure starts to be disclosed on an Ag-deposited Au(111) surface in Figure 5E imaged at 0.006 V. The STM image exhibits a hexagonal array of spots, being quite uniform over the entire area of Ag upon Au-(111). The distance between the spots is measured to be 0.28 ± 0.02 nm, which is the same as the interatomic distance of Au. The atomic rows are also parallel to those of an Au(111) surface. Therefore, the observed structure is assigned to a close-packed (1×1) adlattice of Ag on Au(111). The bright spots have nearly equal heights of ~ 0.02 nm, and three lattice vectors are manifested by arrows and notations in Figure 5E.

3.3.2. STM Imaging of Ag Upd on Au(111) in the Presence of Cl$^-$. Figure 6a shows an atom-resolved STM image in a 0.1 M HClO$_4$ solution with saturated AgCl at 0.4 V. The STM image reveals a constant modulation and an equal distance among spots. The distance between the nearest neighboring atoms is measured to be 0.5 ± 0.05 nm, which is $\sqrt{3}$ times as long as the interatomic distance of Au. The atomic rows of this structure are rotated 30° from those of Au, certified by the 2-dimensional fast Fourier transformation (2-D FFT). Thus, this structure is allotted to a $(\sqrt{3} \times \sqrt{3})$R30° adlayer, and the unit cell is depicted with a rhombus in Figure 6A. Each spot is tentatively assigned to a Ag atom, although the well-known $(\sqrt{3} \times \sqrt{3})$R30° structure of Cu upd on Au(111) in the presence of sulfate is confirmed to be the participation of anions.[36,37] Also,

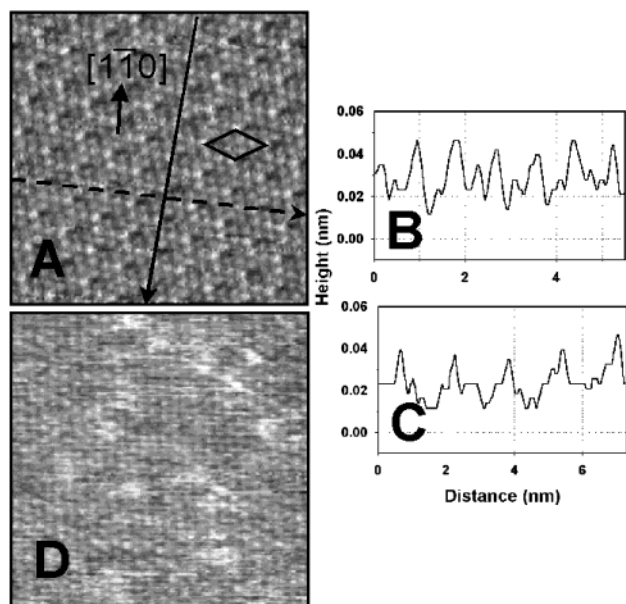(36) Blum, L.; Huckaby, D. A. *J. Electroanal. Chem.* **1994**, *375*, 69.

Figure 7. (A) High-resolution STM image (7.6 × 7.6 nm²) of an Ag adlayer on Au(111) in a solution with saturated AgCl and 0.1 M HClO$_4$ at E = 0.054 V. I_{tip} = 2 nA. E_{bias} = 500 mV. A unit cell is assigned. The profiles taken along a solid-lined (B) and a dash-lined (C) arrow are marked in part A. (D) 8.2 × 8.2 nm² image of an Ag adlayer on Au(111) at E = −0.14 V. I_{tip} = 2 nA. E_{bias} = 700 mV.

this structure was observed at the iodide adsorptions on Ag(111)[38] and on Au(111).[39] In the case of chloride adsorption on Ag(111), however, a double-row structure of Cl was reported.[38] Thus, our STM image of ($\sqrt{3}$ × $\sqrt{3}$)R30° manifests Ag on Au(111).

Figure 6B shows an atomic STM image in 0.1 M HClO$_4$ and saturated AgCl at 0.2 V. The STM image reveals strong modulations and a moiré pattern. The spacing between bright spots is measured to be 1.26 ± 0.05 nm, which is $\sqrt{19}$ times as large as the interatomic spacing of Au. Since the lattice vectors of this structure are rotated 37° from those of an Au(111) surface, this structure is thus appointed to a ($\sqrt{19}$ × $\sqrt{19}$)R37° adlattice, and the unit cell is allotted with a rhombus in Figure 6B. Figure 6C displays a profile of the STM image taken along the solid-lined arrow depicted in Figure 6B. The profile suggests that there are three kinds of atomic sites with the apparent height difference of each modulation above the corresponding basis, evincing that each Ag atom is landed on the different positions. Since a ($\sqrt{19}$ × $\sqrt{19}$)R37° adlattice on Au(111) was not reported at a halide adsorption on Ag(111)[38] and on Au(111),[39,40] the atoms, as shown in Figure 6B, are confirmed to be the Ag atoms on Au(111).

When the potential is stepped to the negative value, the ($\sqrt{19}$ × $\sqrt{19}$)R37° adlayer structure obtained at 0.2 V abruptly disappears, and a new feature on Au(111) is imaged within 5 min. Figure 7A exhibits a newly obtained STM image of Ag upd on Au(111) in the presence of chloride, where the potential is 0.054 V. The spacing between the bright spots is 1.03 ± 0.05 nm, which is $\sqrt{13}$ times larger than the interatomic spacing of Au. The lattice vectors of this structure are deviated ∼46° from those of

the Au(111) atomic rows, observed by 2D-FFT. Thus, this structure is allotted to a ($\sqrt{13}$ × $\sqrt{13}$)R46° adlayer, and the unit cell is manifested with a rhombus in Figure 7A. Figure 7B displays the cross-section along the solid-lined arrow drawn in Figure 7A. The heights of the bright spots are measured to be 0.04 and 0.02 ± 0.01 nm above the corresponding terrace. Figure 7C also shows a line profile that is taken along the dash-lined arrow described in Figure 7A. Each maximum of the corrugation corresponds to the bright spots, where the measured height is 0.04 ± 0.01 nm. Another height difference is 0.02 ± 0.01 nm.

As the potential becomes more negative, a strong moiré pattern is degraded, while another feature begins to appear over the entire area of the Au(111) surface. An STM image that reveals a rough surface and a quasi-hexagonal array of atoms, compared with other atomic images, is shown in Figure 7D, imaged at −0.14 V prior to the very bulky deposition. The distance between the neighboring atoms is measured to be 0.35 ± 0.05 nm, which is 1.2 times as long as the interatomic distance of Au. The lattice vectors of this structure are closely matched to those of an Au(111) surface. Thus, this structure is assigned to a (6 × 6) adlattice. The vertical distance of bright spots, distributed randomly, is measured to be 0.07 ± 0.01 nm. The STM image, as shown in Figure 7D, is hardly found in other reports at the atomic level. One of the main reasons for the formation of this rough structure is the effect of chloride adsorption which is affirmed by the chloride adsorption on Ag(111).[41] Chloride adsorbed on surfaces is considerably mobile, where it makes STM imaging unstable and poorly resolved under this potential region. Compensating the thermal drift of an STM scanner, therefore, we frequently observed the repositioning of bright spots within the acquisition time of one STM image.

4. Discussion

Compared with Ag upd on Au(111) in a pure HClO$_4$ solution, Ag deposition or stripping on Au(111) in the presence of chloride exhibits unique features. Although the low concentrations of silver and chloride are unavoidably employed, Ag adlayer structures on Au(111) explicitly reveal that they are strongly dependent on the chloride adsorption and the electrode potential.

4.1. Growth of Ag on Au(111). There are characteristic features in Ag growth on Au(111) whether chloride is present or not. In the presence of chloride, particularly, the enhanced surface mobility due to chloride adsorption helps the edge decoration and the lateral growth of Ag.

4.1.1. In Perchlorate. After the first peak (C$_1$ in Figure 1) of Ag upd, Ag islands are deposited on Au(111) terraces, and the heights of Ag islands are considerably lower than that of a bulk Ag(111) substrate. As the potential becomes more negative, the lateral growth of Ag controls the whole process of Ag deposition until a monolayer of Ag on Au(111) is accomplished. We also note that the existence of the second Ag adlayer in the underpotential range is associated with the shoulder peak in a cyclic voltammogram. As the potential is stepped to the positive value, terraces and steps of an Au(111) surface appear again. Thus, the adsorption and desorption of Ag are highly reversible, indicating that alloy formation between Ag and Au does not occur during potential cycles.

4.1.2. In Chloride. There are three different stages for Ag growth and a distinct feature for Ag desorption in a chloride-containing solution. The initial stage of Ag nucleation on Au(111) starts at defects that are energeti-

(37) Toney, M. F.; Howard, J. N.; Richer, J.; Borges, G. L.; Gordon, J. G.; Melroy, O. R.; Yee, D.; Sorensen, L. B. *Phys. Rev. Lett.* **1995**, *75*, 4472.
(38) Schott, J. H.; White, H. S. *J. Phys. Chem.* **1994**, *98*, 291.
(39) Gao, X.; Weaver, M. J. *J. Am. Chem. Soc.* **1992**, *114*, 8544.
(40) Tao, N. J.; Lindsay, S. M. *J. Phys. Chem.* **1992**, *96*, 5213.

(41) Aloisi, G.; Funtikov, A. M.; Will, T. *J. Electroanal. Chem.* **1994**, *370*, 297.

cally favorable because of the increased number of bonding sites between an adatom and a substrate. In particular, an STM image manifests that Ag islands are nucleated around the lower portions of Au(111) steps, denoting that the lower step is more stable than the upper step. These nucleated Ag islands are so mobile that they easily move to the step-edge sites of Au and, finally, form bumps at Au steps within the acquisition time of one STM image. This interesting observation suggests that the chloride adsorbed on top of a Ag island enhances the surface mobility. Therefore, a bilayer structure between Ag and Cl can be conceived, which is supported by a much higher topography of Ag islands (0.34 ± 0.02 nm) under this condition. At the potential -0.12 V, the more fascinating Ag structure manifests only at the Au step-edge sites. Although the edge decoration occurs in low concentrations of silver ions in the absence of chloride, equally distributed Ag islands are observed only in a saturated AgCl solution. Thus, chloride plays a crucial role in the edge decoration, where the width and the height of them are measured to be ~10 and 0.35 nm, respectively. As the potential becomes more negative, Ag islands cover the entire surface of an Au substrate, and laterally overgrown steps begin to emerge. These are consecutive processes of Ag growth in the presence of chloride that have a significant influence on the increase of surface mobility verified with the formation of bumps by way of step-flow growth, as shown in Figure 4E.

In contrast to Ag deposition, the desorption of Ag in a chloride-containing solution yields particle-like AgCl, which firmly adheres to an Au(111) surface, and complete stripping of the sticky AgCl requires additional overpotential that makes the whole process of Ag adsorption or desorption quite irreversible. Chloride adsorption on the Ag overlayer upon Au(111) also causes the formation of streaky steps and the fluctuation of steps during a desorption process. As in previous works, noticeable step fluctuation due to chloride adsorption on Au(111)[30] and on Ag(111),[31] in which the driving force is the edge diffusion, closely coincides with our observations. Therefore, the deposition and the desorption of Ag on an Au-(111) substrate are definitely influenced by chloride ions.

4.2. Structural Changes. *4.2.1. In Perchlorate.* After the first upd of Ag, an STM image reveals a (4×4) structure over the entire surface. Although perchlorate is well-known as a weakly adsorbed anion, the formation of an open adlattice elucidates the participation of anions by repulsive forces in the overlayer structure. Figure 8A shows a ball model of a (4×4) adlayer structure corresponding to the surface coverage 0.56, which is approximately matched to the surface coverage 0.42 acquired from electrochemical measurement. As the potential becomes near the second upd of Ag, a closely packed (1×1) structure starts to manifest on the Ag layer upon Au(111). Because the interatomic distance of Ag is in good agreement with that of Au, this can be interpreted as a model system of a (1×1) structure.

4.2.2. In Chloride. There are four characteristic structures which are clearly matched to features in a cyclic voltammogram shown in Figure 2. Around the C_1 peak, an STM image reveals an open ($\sqrt{3} \times \sqrt{3}$)R30° adlattice. A ball model has the surface coverage 0.33 which is much higher than that obtained from a coulometric curve (0.03). This discrepancy might be originated from two possible sources. One is the difference of the potential of zero charge (pzc); an Au(111) electrode changes to more negative values during Ag deposition because the pzc values of Au(111)
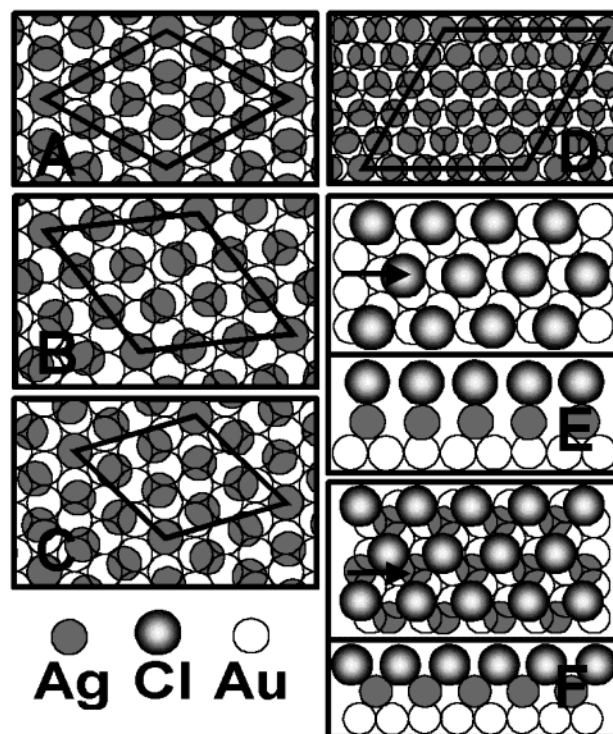

Figure 8. Atomistic models of the Ag adlayer on Au(111). Gray circles are silver, degraded circles are chloride, and open circles are gold. (A) (4×4) structure. (B) ($\sqrt{19} \times \sqrt{19}$)R37° structure. (C) ($\sqrt{13} \times \sqrt{13}$)R46° structure. (D) ($6 \times 6$) structure. (E) Suggested bilayer structure between Ag and Cl based on ($\sqrt{3} \times \sqrt{3}$)R30° structure. Top: top view (an arrow indicates the direction of a side perspective). Bottom: side view. (F) Another model of the bilayer structure. Top: top view (an arrow denotes the direction of a side perspective). Bottom: side view.

and Ag(111) differ by 1 V.[42] The other is the anodic charge that is consumed to adsorb chloride ions over the Au(111) substrate or Ag adatoms. Although we did not quantify an accurate amount of chloride adsorption with the STM, which is short of information about chemical identities, the existence of anodic charge was easily recognized as the step fluctuation and the increased surface mobility were observed. As another aspect, bond formation between Ag and Cl is a spontaneous process because Au−Cl (-34.7 kJ/mol) and Ag−Cl (-127 kJ/mol) have negative values, on the basis of the formation enthalpies for metal salts.[43] Additionally, thermal desorption experiments of Bowker et al. demonstrated that Cl and Ag formed strongly bound complexes which closely resembled AgCl.[44] Therefore, the anodic charge due to the chloride adsorption must be compensated, and these sources cause the difference of surface coverage between an STM image and a coulometric curve.

As the potential becomes more negative around the peak C_2, a ($\sqrt{19} \times \sqrt{19}$)R37° adlattice appears over the entire surface. A ball model that has the surface coverage 0.49, which is still higher than that from a coulometric curve (0.21), is shown in Figure 8B. The strong moiré pattern of a ($\sqrt{13} \times \sqrt{13}$)R46° adlattice begins to appear over the Au(111) surface after the C_2 peak. A ball model that possesses the surface coverage 0.55 is depicted in Figure 8C. However, the charge density conforms to the surface coverage 0.32, which is approximately half of the value

(42) Valette, G. *J. Electroanal. Chem.* **1989**, *269*, 191.
(43) West, R. C. *Hanbook of Chemistry and Physics*; CRC Press: Boca Raton, FL, 1992.
(44) Bowker, M.; Waugh, K. C. *Surf. Sci.* **1983**, *134*, 639.

expected from the ball model. At a potential near the bulk deposition posterior to the peak C_4, a (6 × 6) structure starts to emerge. Figure 8D shows a ball model that points out the surface coverage 0.69, denoting that a complete monolayer of Ag is not formed within the underpotential range. Thus, a close-packed (1 × 1) overlayer of Ag is accomplished at −0.48 V, which is the region to fairly pass the bulk deposition. Even if the surface coverage between an electrochemical measurement and STM image shows a different behavior, unique features of a cyclic voltammogram are relevant to the phase transition of Ag on Au(111) for each adlayer structure acquired from STM images in the presence of chloride.

As another aspect, Ag atoms are capped with chloride anions that are easily adsorbed upon a Ag atom on Au-(111), similar to previous results of Ag upd on iodine-modified Au(111)[45] and Cu upd on iodine-modified Pt-(111),[46] indicating a bilayer structure composed of both Ag and Cl. Also, the high topography of Ag islands, as shown in Figure 4A, validates the landing of chloride anions on Ag atoms upon Au(111). We note that two kinds of bilayer structures are possible. One includes the direct binding of chloride on a Ag adatom in which the chloride anions are packed on atop sites of Ag atoms. This bilayer structure is shown in Figure 8E, depicted on the ($\sqrt{3}$ × $\sqrt{3}$)R30° structure as a side view and a top view. The other includes the positioning of chloride at a 3-fold site among Ag atoms, and Figure 8F depicts it as a side view and a top view. On the basis of the formation enthalpies of metal salts, the second structure is more favorable than

the first one, since the system acquires the energetic gain of −254 kJ/mol by the formation of two additional Ag−Cl bonds. However, the definitive assignment of the bilayer structure must be studied further.

5. Conclusion

We conducted electrochemical and STM measurements to elucidate the process of Ag growth and the structures of Ag upd on Au(111) when chloride anions were present or absent. In the absence of chloride, an open (4 × 4) structure transforms into a close-packed (1 × 1) overlayer structure, and the system of Ag upd is reversible. In contrast to this, the introduction of chloride anions leads to distinctive features being exhibited in the cyclic voltammograms and STM images of Ag upd on Au(111). We observed four different structures of Ag on Au(111) in a chloride-containing solution as a function of potential and as a function of chloride adsorption in which ($\sqrt{3}$ × $\sqrt{3}$)R30°, ($\sqrt{19}$ × $\sqrt{19}$)R37°, ($\sqrt{13}$ × $\sqrt{13}$)R46°, and (6 × 6) adlayer structures are ascertained at each potential realm. These structures suggest that chloride anions strongly interact with Ag atoms during the upd process, and therefore, chloride plays an important role in the structure of a Ag adlayer on Au(111). Currently, we anticipate further research on the less investigated upd systems in the presence of anions in spite of the low solubility of metal salts (AgF, AgBr) in aqueous solutions.

(45) Sugita, S.; Abe, T.; Itaya, K. *J. Phys. Chem.* **1993**, *97*, 8780.
(46) Inukai, J.; Osawa, Y.; Wakisaka, M.; Sashikata, K.; Kim, Y.-G.; Itaya, K. *J. Phys. Chem. B* **1998**, *102*, 3498.